NONLINEAR REFRACTION AND INCREASING ABSORPTION IN HgCdTe OPTICAL BISTABILITY AT ROOM TEMPERATURE: AN EXPERIMENTAL STUDY

S. CECCHI, P.M. COPPO, P. SALIERI and F.T. ARECCHI
Istituto Nazionale di Ottica, Largo E. Fermi 6, 50125 Firenze, Italy

Received 7 December 1987

The effects of nonlinear absorption in optical bistability as observed at room temperature in $Hg_{0.815}Cd_{0.185}Te$ samples are investigated. As intensity is increased, a new feature for HgCdTe is observed, namely the transition in transmission from anticlockwise hysteresis loops. This transition is not present in reflection. Our observations are consistent with the assumption of thermally induced changes in the nonlinear optical properties of the semiconductor.

1. Introduction

The alloy semiconductor $Hg_{1-x}Cd_xTe$ is a very important material for infrared detection. Its bandgap energy E_g can be tuned from 0 to 1.6 eV by varying its mole fractions x [1]. This fact has led in the last few years to many experiments in which the large band gap resonant optical nonlinearities have been matched in energy to specific infrared laser sources and in particular to the CO_2 laser.

Many authors have experimentally examined the refractive nonlinearities of HgCdTe [2]: in particular Miller and his group have carried out a series of experiments, in which optical bistability has been investigated under different conditions [3]. Bandgap resonant nonlinearities of electronic origin are weak at room temperature, because the Auger carrier recombination rate strongly increases with temperature [4]. Thus they are masked by thermally induced nonlinearities. Thermal effects are of special interest in HgCdTe since, as observed in PbSnSe [5] and untypically for a zincblende compound, heating the crystal gives the same sign of refractive index change as the electronic contribution [6].

In this communication we extend the analysis of Craig et al. on thermally induced room temperature optical bistability at low incident power levels [7]: we show, for the first time in HgCdTe, the appearance of clockwise hysteresis cycles in transmission as the incident intensity is increased, due to thermally induced nonlinear absorption. We can account for both absorptive and refractive nonlinear contributions by simultaneous monitoring of the sample transmission and reflection.

We will then present numerical results obtained by a computer program which, using the absorption characteristics that we measured after AR coating one face of the sample under investigation, parametrically solves the nonlinear Fabry Perot equations. This simulation also accounts for the switching overshoot phenomenology, observed in both dispersion and absorption dominated regimes. The measured absorption curves are then discussed with reference to a possible nonlinear free carrier contribution.

2. Experimental observations

A set of $Hg_{0.815}Cd_{0.185}Te$ plates with thickness $D=280$ μm, was prepared for us by Elettronica SpA, Rome, by cutting slices of lingots (1 cm in diameter) composed of an ensemble of monocrystals: the presence of different domains could also be detected by visual inspection. The surface of the samples had been later mechanically polished in order to form a Fabry Perot etalon and cleaned in methanol. The material is p doped with the nominal concentration typical of the crystal as grown ($p_a=1\times10^{16}$ cm^{-3}).

We used a single mode CO_2 laser (Linelite model 941) actively intensity and frequency stabilized. A

0 030-4018/88/$03.50

small fraction of the beam (1%) is split on a photovoltaic detector to monitor the incident intensity. The input beam is focused on the sample by a 14 cm lens (all optics being properly Ar coated) to a 400 μm spot diameter. The micropositioning of the sample on the focal plane could be controlled by observing in reflection the distance at which the same lens would image the sample. The transmitted portion of the beam is then collected by a 3 cm focal length lens onto a 0.1 cm^2 pyroelectric detector. The portion reflected by the sample is also monitored by a pyroelectric detector. These signals are then synchronously detected, to be later digitized and stored or displayed on a chart recorder. The reading of all detectors was calibrated in absolute power.

The samples under investigation were placed in a thermally controlled environment, supported by three holders without heatsinking at the center of a cylindrical cell in copper, around which a properly insulated heating resistor is wound. Two holes were drilled in the lateral plexiglass windows to allow for passage of the laser beam. A precision platinum resistor is placed within the cell for precise measurement of the temperature of the air, which acts as thermal bath for the sample. An active thermal control system has been designed in order to stabilize both transients and long term drifts [8]. As the transitions between stable states were observed to take place over a time scale of the order of a second, the laser intensity incident on the sample was scanned very slowly (20–30 min), in order to allow the sample to thermalize at each successive increment. Bistability was observed over a rather broad range of frequencies in the 10.6 μm band. In fig. 1a the low intensity absorption profile of the sample (after AR coating) is shown as measured with a Perkin Elmer model 727B infrared spectrometer: we indicate the nominal band gap wavelength [9] and two wavelengths at which the laser was typically operated. From these measurements we have calculated an absorption coefficient as a function of energy as shown in fig. 1b: the observed exponential dependence agrees with the Urbach's law predicted for absorption in the band tail [6]. In fig. 2 we show a typical set of measured transmission and reflection curves. The three sets of data differ in zero intensity cavity mistuning, which was varied by minor translations of the sample in front of the beam, making use of the non perfect parallelism of its faces. At power levels

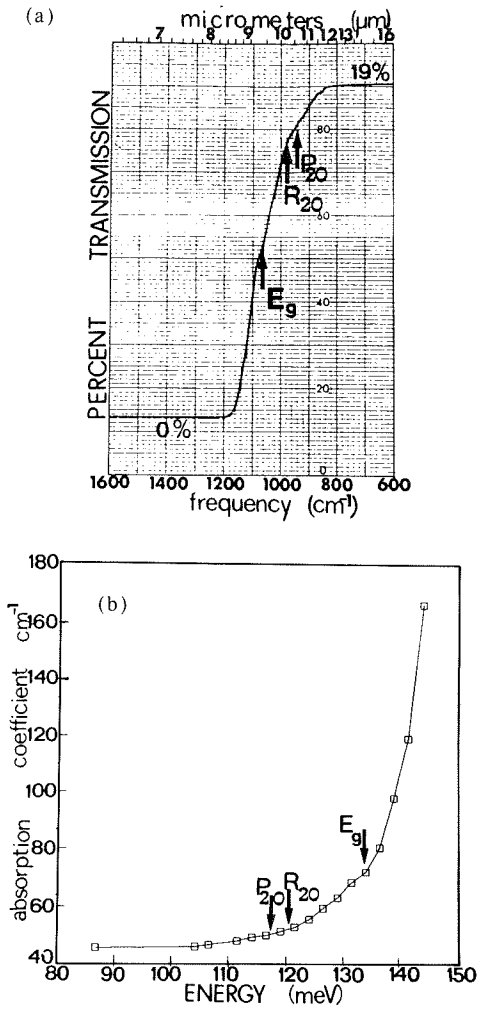

Fig. 1. (a) Transmission of a $Hg_{0.815}Cd_{0.185}Te$ plate, AR coated on its rear face, as a function of frequency. (b) Absorption coefficient α as a function of photon energy.

below 70 mW the observed behavior as intensity is increased, with counterclockwise (ccw) hysteresis cycles in transmission and clockwise (cw) cycles in reflection, is characteristic of dispersive bistability. At higher power levels the non linear increase in absorption induces a different phenomenology (cw cycles are observed both in transmission and in reflection).

The thermal origin of the nonlinearities is confirmed by additional measurements performed using a different sample support, in which heat sinking was provided by two copper annular holders in direct contact with both sides of the sample: the measured

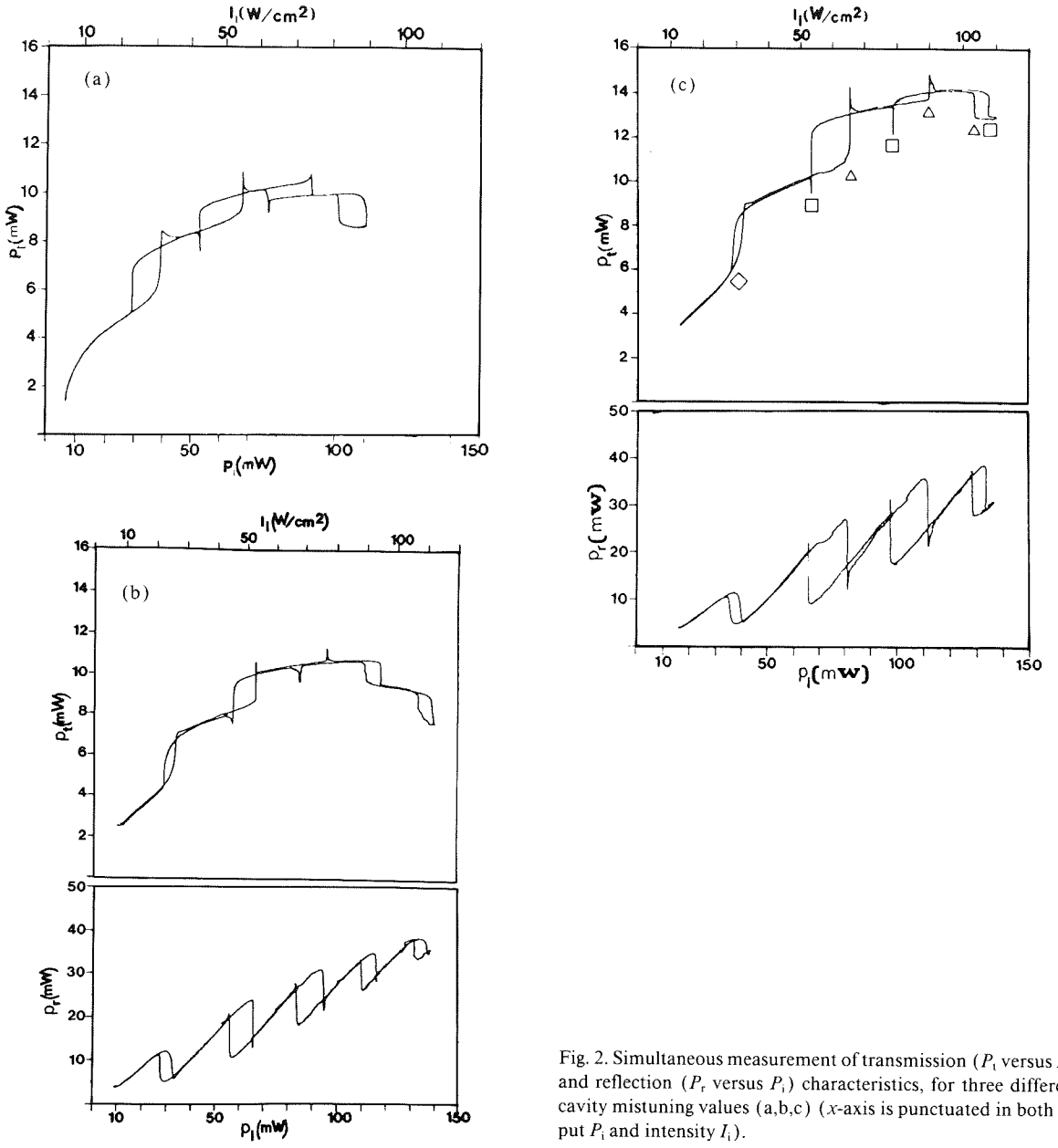

Fig. 2. Simultaneous measurement of transmission (P_t versus P_i) and reflection (P_r versus P_i) characteristics, for three different cavity mistuning values (a,b,c) (x-axis is punctuated in both input P_i and intensity I_i).

transmission and reflection data are very similar to those of fig. 2, but correspond to higher power and to switching times reduced by a factor of two [8].

3. Discussion

The induced thermooptic effect was measured directly and indirectly. With the laser beam impinging at the center of the sample at an intensity held close to the first cw cycle switchdown in transmission, a set of contact temperature measurements was performed at constant thermal bath temperature (30°C) by way of a micrometrically positioned Cu-Sn thermocouple. These measurements indicated the existance of a strong temperature gradient on the sample:

the temperature was measured to increase from 33°C at 2 mm away from the edge to 40°C, at 1 mm closer to its center. We did not move the sensor closer to the center to avoid possible false reading induced by absorption of the heat conducting paste at the junction tip. The laser induced heating was measured at the center of the sample by use of a close focus optical thermometer with 2 mm resolution (Cyclops 33CF), calibrated with reference to the thermal bath with the input beam blocked off. With the beam on, the whole sample, slightly tilted to avoid possible reflections, was scanned, operating the optical pyrometer in a peak mode. In the center a maximum induced temperature increase $\delta T = 27°C$ was measured. A set of transmission and reflection measurements (summarized in fig. 3a) was then performed at different thermal bath temperatures keeping the position of the beam on the sample fixed. As temperature is increased, the position of the hysteresis cycles associated with a given cavity interference order moves to lower power, as shown in fig. 3a from which a value of $dn/dT = -2.8 \times 10^{-3}\ K^{-1}$ can be deduced. The whole temperature increase associated with an input intensity scan (as in fig. 2) has been inferred from fig. 3b to be 30–35°C, with steps of 2.5–3.5°C at the switching points.

In order to determine the intrinsic nonlinear features of the material absorption we had the rear face of the sample AR coated: at a thermal bath temperature of 30°C we measured a low intensity reflectivity at normal incidence $R = 0.32$, corresponding to $n = 3.65$, and a transmission curve as shown in fig. 4a. The material absorption coefficient α obtained from simultaneous reflection and transmission data is given in fig. 4b (i as function of the power absorbed by the sample P_a, which is proportional to the induced temperature difference δT.

We numerically modeled the observed behavior of our system using the equations that describe a non linear Fabry-Perot:

$$P_t = [(1-R)^2 A\,(1-AR)^2] \times P_i / \{1 + [4AR/(1-AR)^2] \sin^2 \Phi\}\,,$$

$$P_c = \{(1+AR)\,[(1-A)/(1-R)]\,(-A \ln A)\}\,P_t\,,$$

$$P_r = P_i - P_t - \alpha D\,P_c\,, \qquad (1)$$

where P_i, P_t, P_c, P_r indicate the input, transmitted, cavity and reflected powers, $A = \exp(-\alpha D)$ the integrated one pass absorption. The induced nonlinear phase shift Φ is assumed to be proportional to P_a as for a thermal nonlinearity ($\Phi = f_0 + f_1 P_a$): this is con-

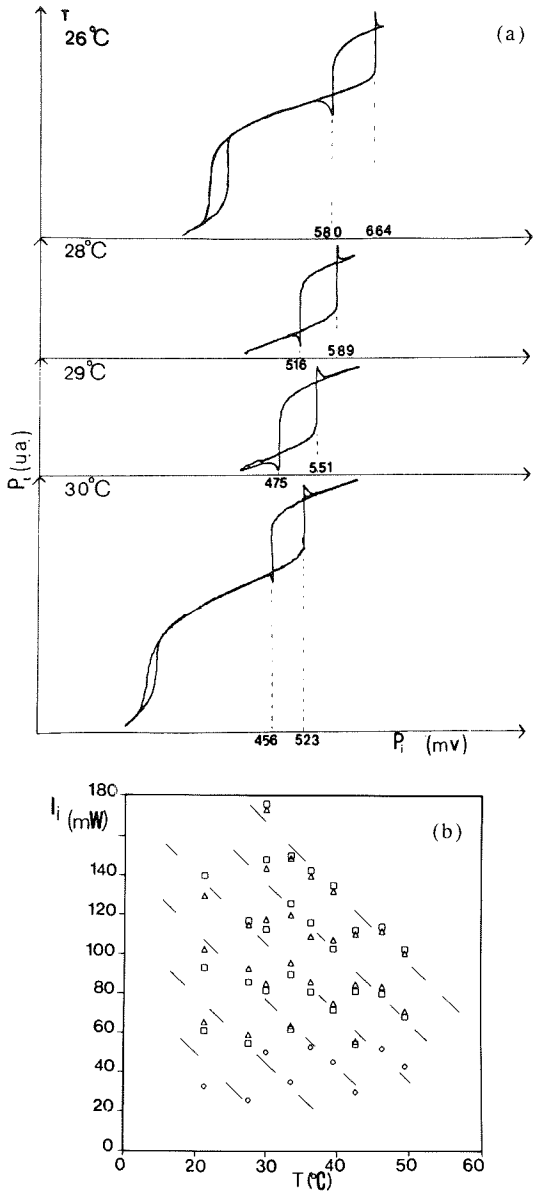

Fig. 3. (a) Shift of an hysteresis cycle towards lower input powers (as expected for $dn/dT < 0$) as the temperature of the bath T is increased (1 mV = 0.124 mW). (b) Shift with thermal bath temperature T of the nonlinearities associated to different cavity orders as observed in transmission: as shown in fig. 2c ◇ indicates the input power (P_i) corresponding to the first hysteresis cycle (always found to be relatively narrow), △ the value corresponding to a switchup and □ the value corresponding to a switchdown in the following cycles.

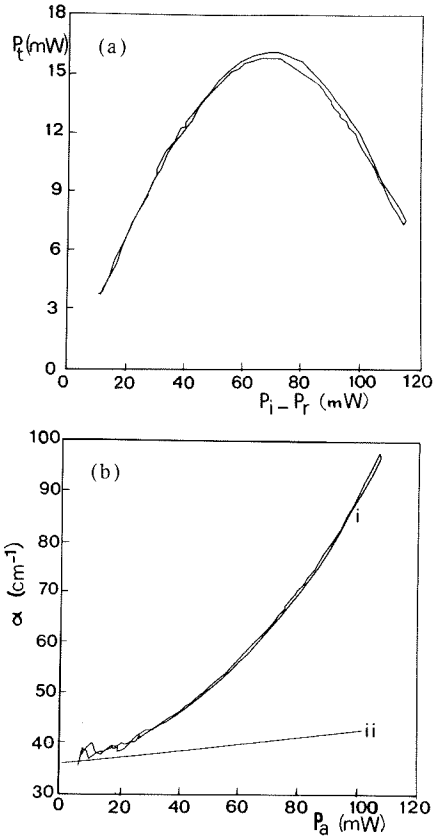

Fig. 4. (a) Transmission function of a sample AR coated on its rear face ($\lambda = 10.24\ \mu m$): P_t = transmitted power, P_i = input power, P_r = reflected power. (b) Absorption coefficient as a function of the absorbed power P_a: (i) measured (ii) calculated according to eq. (3).

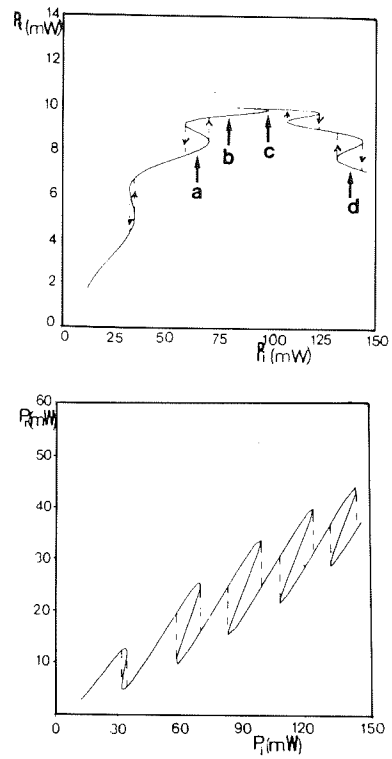

Fig. 5. Calculated transmission and reflection characteristics (to be compared with fig. 2b).

sistent with our observations (see fig. 2) which indicate that the spacing between hysteresis cycles is progressively reduced as P_i is increased. Eqs. (1) were rewritten expressing P_t and P_i as functions of P_a ($P_a = \alpha D\, P_c$) and solved by iterating P_a, using as input for the calculation the absorption measurements of fig. 4, an initial phase shift $f_0 = -0.38\ \pi, f_i = -0.04$ rad/mW as indicated by our reflection measurements (fig. 2): the calculated curves are shown in fig. 5. They must be compared with the corresponding experimental data of fig. 2b. Eqs. (1) can also be written as

$$P_t/P_i = [(1-R)^2 A/(1-AR)^2] \times \{1 + [4AR/(1-AR)^2] \sin^2(\Phi)\}, \qquad (2')$$

$$P_t/P_i = \{(1-R)\ [A/(1+AR)]\ (1-A)\}\ (P_a/P_i)\,, \qquad (2'')$$

in order to apply a graphical method of solution [10] (fig. 6).

We have indicated four values of input power, which, at the intersections of (2′) and (2″), correspond to one or more solutions, with different stability properties. Points where the slope of the Airy function (2′) is less than that of the curve (2″) are stable stationary solutions: this applies also to the case where (point e in fig. 6) both slopes are negative and a cw hysteresis loop is obtained in transmission.

As the system dynamics is governed by the slow medium nonlinearities during the switchings, the system evolves following the cavity function (2′). Fig. 6 explains the overshoots (clearly present also in our reflection measurements) observed in the switchups and switchdowns in both ccw and cw cycles. Only at the highest input powers the induced cavity finesse reduction smoothens and eventually quenches this feature, as observed. At the third interference order, while the transient features remain essentially unaffected, in transmission the shape of the hysteresis cycle can be drastically modified (as

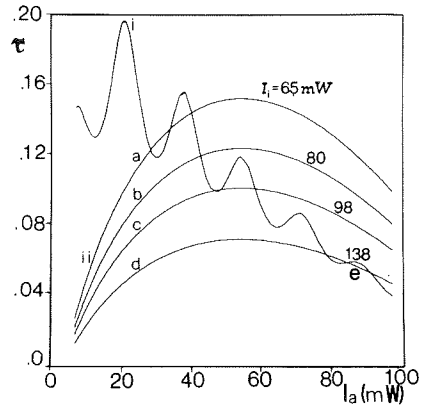

Fig. 6. Graphical solution for eqs. (2): four values of input powers are shown with a, b, c, d corresponding to the same values indicated in fig. 6: stable solutions correspond to intersections where the slope of (i) is less than (ii).

shown in fig. 2 with a transition from a ccw to a cw cycle) by a suitable choice of the cavity mistuning and the two possible transmission states can be seen of the same height: the effect can be explained assuming in fig. 6 different initial phase shifts for the Airy function (2′). The measured increase in absorption with power (already present in the observations of ref. [7], though in a lesser degree) is not easy to interpret: indeed, for $x=0.185$, dE_g/dT is known to be positive and therefore the observed quasi exponential increase of the absorption coefficient (fig. 4b (i)) cannot be attributed to band tail absorption in presence of a shrinking band gap. If we tentatively attribute this effect to an increase with temperature of free carrier absorption we can write the absorption coefficient temperature dependence, time scales being sufficiently long for the carriers to thermalize under constant irradation, as

$$\alpha(T)=\alpha_0+\sigma_n P_0(T)+\sigma_n N_0(T)\,, \qquad (3)$$

where $\alpha_0=17\ \mathrm{cm}^{-1}$ is the background absorption, $\sigma_p=3.0\times10^{16}$ and $\sigma_n=0.867\times10^{16}\ \mathrm{cm}^2$ [11] indicate the intraband absorption cross sections for holes and electrons, $N_0(T)=[(P_a^2+4N_i^2)^{1/2}-P_a]/2$ and $P_0(T)=[(P_a^2+4N_i^2)^{1/2}+P_a]/2$ are the carrier concentrations at equilibrium (cm^{-3}), $N_i(T)=(1.093-0.296\,x+0.442\times10^{-3}\,T)\times5.16\times10^{14}\times E_g^{+3/4}\,T^{3/2}\exp(-E_g/2k_bT)$ being the intrinsic concentration [12], $E_g(T)=-0.302+1.93\,x+5.35\times10^{-4}\,(1-2x)\,T-0.81\,x^2+0.832\,x^3$ eV [9], k_b(eV/K) is the Boltzmann constant. The calculated absorption coefficient is shown in fig. 4b (ii): bigger cross sections are required to fit our experimental data, at least within the temperature range that we have explored ($\sim$30–65°C).

In conclusion, we have reported on an investigation of the nonlinear transmission and reflection properties of HgCdTe plates, extended to power levels at which the effect of increasing absorption drastically modifies the features of hysteresis cycles in transmission, while in reflection they remain essentially unchanged. These observations are explained in terms of a non linear effect of thermal origin: we have measured a thermooptic coefficient ($dn/dT=-2.8\ \mathrm{K}^{-1}$) nearly three times bigger than previously reported. The origin of the observed increasing absorption is however at present not yet understood and requires further investigations.

Acknowledgements

We thank G. Giacomelli for his assistance. This study was conducted in the framework of the European Joint Optical Bistability Project (EJOB) of the Commission of the European Communities.

References

[1] D. Long and J.L. Schmit, Semiconductors and Semimetals, Vol. 5, eds. R.K. Willarson and A.C. Beer (Academic Press, New York, 1970) p. 175.
[2] R.K. Jain and D.G. Steel, Optics Comm. 43 (1982) 72.
[3] A. Miller and G. Parry, Phil. Trans. R. Soc. Lond. A 313 (1984) 277.
[4] P.E. Petersen, Semiconductors and Semimetals, Vol. 18, eds. R.K. Willarson and A.C. Beer (Academic Press, 1981) p. 121.
[5] J.J.E. Reid, A.K. Kar, H.A. McKenzie, R. Grisar and H.M. Preier, Optics Comm. 64 (1987) 175.
[6] E. Finkman and Y. Nemirowski, J. Appl. Phys. 50 (1979) 4356.
[7] D. Craig, M.R. Dyball and A. Miller, Optics Comm. 54 (1985) 83.
[8] S. Cecchi, P.M. Coppo and P. Salieri, to be published in Nuovo Cimento D.
[9] G.L. Hansen, J.L. Schmit and T.N. Casselman, J. Appl. Phys. 53 (1982) 7099.
[10] F.S. Felber and J.H. Marburger, Appl. Phys. Lett. 28 (1976) 731.
[11] J.A. Mroczkowski and D.A. Nelson, J. Appl. Phys. 54 (1983) 204.
[12] J.L. Schmit, J. Appl. Phys. 41 (1970) 2876.